Can primordial parity violation explain the observed cosmic birefringence?

Tomohiro Fujita[*]
Waseda Institute for Advanced Study, Shinjuku, Tokyo 169-8050, Japan
and Research Center for the Early Universe, The University of Tokyo, Bunkyo, Tokyo 113-0033, Japan

Yuto Minami
Research Center for Nuclear Physics, Osaka University, Ibaraki, Osaka 567-0047, Japan

Maresuke Shiraishi
School of General and Management Studies, Suwa University of Science, Chino, Nagano 391-0292, Japan

Shuichiro Yokoyama
Kobayashi Maskawa Institute, Nagoya University, Chikusa, Aichi 464-8602, Japan
and Kavli IPMU (WPI), UTIAS, The University of Tokyo, Kashiwa, Chiba 277-8583, Japan

(Received 25 September 2022; accepted 14 November 2022; published 28 November 2022)

Recently, the cross-correlation between E- and B-mode polarization of the cosmic microwave background, which is well explained by cosmic birefringence with rotation angle $\beta \approx 0.3$ deg, has been found in cosmic microwave background polarization data. We carefully investigate the possibility of explaining the observed EB correlation by the primordial chiral gravitational waves, which can be generated in the parity-violating theories in the primordial Universe. We found that the chiral gravitational wave scenario does not work due to the overproduction of the BB autocorrelation, which far exceeds the observed one by SPTPol and POLARBEAR.

DOI: 10.1103/PhysRevD.106.103529

I. INTRODUCTION

Measurements of linear polarization patterns of the cosmic microwave background (CMB) have provided rich information of our Universe [1–9]. The CMB photons gained the linear polarization at the last scattering surface (LSS) at redshift $z \approx 1100$. In addition, the polarization pattern may have been affected by some interactions, which the CMB photons experienced during the travel to observers. The linear polarization patterns of CMB can be decomposed into two orthogonal components: parity even E mode and parity odd B mode. Having them, we can construct two parity even correlations, EE and BB, and a parity odd correlation, EB. If the parity symmetry is conserved for the CMB photons, then the EB cross-correlation should vanish, and thus it is a good probe of parity-violating physics.

Recently, a hint of parity violation was measured in the EB correlation of the CMB photons [10–12], where a parity-violating physics, so-called cosmic birefringence was assumed. Cosmic birefringence is that the linear polarization plane of the CMB photons rotates by angle β while they travel between the LSS and observers. This rotation produces a nonzero EB cross-correlation from EE and BB spectra generated at the LSS as $C_\ell^{EB,\mathrm{obs}} = \sin(4\beta)(C_\ell^{EE} - C_\ell^{BB})/2$ [13]. The recent careful data analysis indicates $\beta \approx 0.3$ deg with about 3σ significance [12]. No significant dependence of β on the CMB photon frequency was found [14]. To explain this cosmic birefringence, several models have been proposed [15–20].

However, the nonzero detection of the EB correlation does not necessarily imply that this parity-violating signal was caused by cosmic birefringence. It is important to consider whether an alternative explanation is possible or not. Primordial chiral gravitational waves (CGWs) are known to produce EB correlation before the LSS because their imbalance between right- and left-handed circular polarization mode breaks the parity symmetry [21]. A number of models, which generate CGWs with various spectrum shapes in the primordial Universe, have been studied [22–33]. It is apparently possible to reproduce the observed EB spectrum $C_\ell^{EB,\mathrm{obs}}$ by considering CGWs with a suitable spectrum shape.

In this short paper, we investigate if CGWs can consistently explain the observed EB spectrum. To test the EB spectrum induced by CGWs with the observed EB, one needs to reestimate the miscalibration angles of detectors, which are simultaneously determined in the measurements of β [10–12]. Because CGWs produce not only the EB

[*]tomofuji@aoni.waseda.jp

spectrum but also the other spectra between T, E, B, an appropriate likelihood function that includes all spectra produced by CGWs is required, which is a very complicated task. However, we have noticed that the induced BB spectrum becomes much larger than the observed value in the CGW scenario. Therefore, we adopted a strategy of focusing on the compatibility of the EB and BB spectra induced by CGWs, which are tuned to mimic the cosmic birefringence signal of $\beta = 0.3$ deg. We do not specify the generation mechanism of CGWs but introduce a spectrum template of CGWs with a sufficient number of parameters to obtain the desired EB spectrum. We shall show that such CGWs lead to the overproduction of the BB spectrum.

This paper is organized as follows. In Sec. II, we introduce our template of CGWs. In Sec. III, we tune the parameters of the CGW spectrum and obtain the EB spectrum similar to the observed one. In Sec. IV, we compute the BB spectrum induced by the CGW spectrum and show that it exceeds the observed value. Section V is devoted to summary and discussion.

II. CHIRAL GRAVITATIONAL WAVES

CGWs, which violate the parity symmetry, produce EB cross-correlation in the CMB polarization anisotropy if they are generated before the recombination era. In this section, we introduce our parametrization of the primordial spectrum of CGWs and illustrate how they induce CMB polarization correlations.

CGWs can be generated in the early Universe in various models, which predict diverse CGW spectrum shapes [22–33]. In this paper, however, we adopt a model-independent approach. We consider fully chiral and log-normal spectra of primordial CGWs and superpose them with different heights and peak positions as

$$\mathcal{P}_h^L(k) \simeq 0,$$
$$\mathcal{P}_h^R(k) = \mathcal{P}_\zeta \sum_i r_i \exp\left[-\frac{1}{2\sigma^2}\ln^2\left(\frac{k}{k_i}\right)\right], \tag{1}$$

where $\mathcal{P}_h^{L/R}$ denotes the dimensionless power spectrum of the left-/right-handed circular polarization modes of the primordial gravitational waves on superhorizon scales. $\mathcal{P}_\zeta = 2.2 \times 10^{-9}$ is the curvature power spectrum on the CMB scale. r_i, k_i, σ parametrize the amplitude, peak scale, and width of $\mathcal{P}_h^R$, respectively. Our template (1) can accommodate a sufficiently large parameter space to try mimicking the observed EB spectrum, though we only introduce the single parameter σ to control the width for simplicity. It should be stressed that we do not propose Eq. (1) as a natural spectrum shape of CGWs. Instead, we will show that even such a highly fine-tuned spectrum fails to explain the observation, and hence it is even harder for more realistic spectra. Note that we consider the parity violation with $\mathcal{P}_h^R \gg \mathcal{P}_h^L$ so that CGWs induce positive EB cross-correlation, which is favored by the measurements [10–12].

Primordial CGWs produce all of the auto- and cross-correlations between the CMB temperature T and linear polarization E and B. Among them, we focus on EB and BB angular power spectra in this paper. The contributions from the CGWs to them are written as, e.g., [26,34,35]

$$C_\ell^{EB} = 4\pi \int \mathrm{d}(\ln k)[\mathcal{P}_h^L(k) - \mathcal{P}_h^R(k)]\Delta_\ell^E(k)\Delta_\ell^B(k),$$
$$C_\ell^{BB} = 4\pi \int \mathrm{d}(\ln k)[\mathcal{P}_h^L(k) + \mathcal{P}_h^R(k)]\Delta_\ell^B(k)\Delta_\ell^B(k), \tag{2}$$

where $\Delta_\ell^{E/B}(k)$ is the tensor transfer function of the CMB E/B mode, and the contributions from the scalar and vector modes are ignored. Since C_ℓ^{EB} and C_ℓ^{BB} are linear functions of $\mathcal{P}_h^R$, each term in our template (1) independently contributes to them.

III. REPRODUCING EB SPECTRUM

In this section, we numerically compute the EB spectrum, which is contributed by the CGWs parametrized in Eq. (1), using a modified version of a publicly available Boltzmann code CAMB [36,37] where Eq. (2) is implemented. We shall fix the parameters, k_i, r_i and σ in Eq. (1), in order to maximally mimic the observed EB spectra.

In Fig. 1, we plot $D_\ell^{XY} = \ell(\ell+1)C_\ell^{XY}/(2\pi)(XY = EB, BB)$, and the left panel is for the EB spectrum and the right panel shows the BB spectrum. In the left panel, the black solid line represents the target EB spectrum inferred by the birefrigence angle reported by Refs. [10–12]. While it is not the observed EB data itself, it suffices for the clear explanation of our claim. One observes that the target EB has five peaks up to $\ell \sim 1500$, which is the $\ell_{\max}$ used in the measurements of β [10–12,14], that inherits from the intrinsic EE spectrum, as cosmic birefringence induces, $C_\ell^{EB,\mathrm{obs}} \simeq \sin(4\beta)C_\ell^{EE}/2$. The colored lines denote the calculated EB spectra produced by the CGWs. In mimicking the target EB with CGWs, we introduce five terms in $\mathcal{P}_h^R$ to individually fit these peaks. To obtain narrow EB peaks from the CGWs, we first set the width parameter to a small value $\sigma = 0.2$, while we will vary it later. Then, we search for the value of the peak scale k_i and the peak amplitude r_i, to ensure that the calculated EB spectrum is adjusted to the position and the height of each peak in the target EB. In this manner, we determine five sets of parameters as $\{k_i\mathrm{Mpc}, r_i\} = \{9.60\times10^{-3}, 5.68\}$, $\{2.82\times10^{-2}, 8.02\times10^{2}\}$, $\{5.00\times10^{-2}, 5.50\times10^{3}\}$, $\{8.70\times10^{-2}, 4.80\times10^{4}\}$, $\{1.10\times10^{-1}, 1.02\times10^{5}\}$. One observes that these EB spectra induced by the CGWs show faster damped oscillations than the target one due to a distinctive feature of the tensor transfer function. Note that their peak position and height do not completely coincide with the target peaks, because they are very sensitive to the free

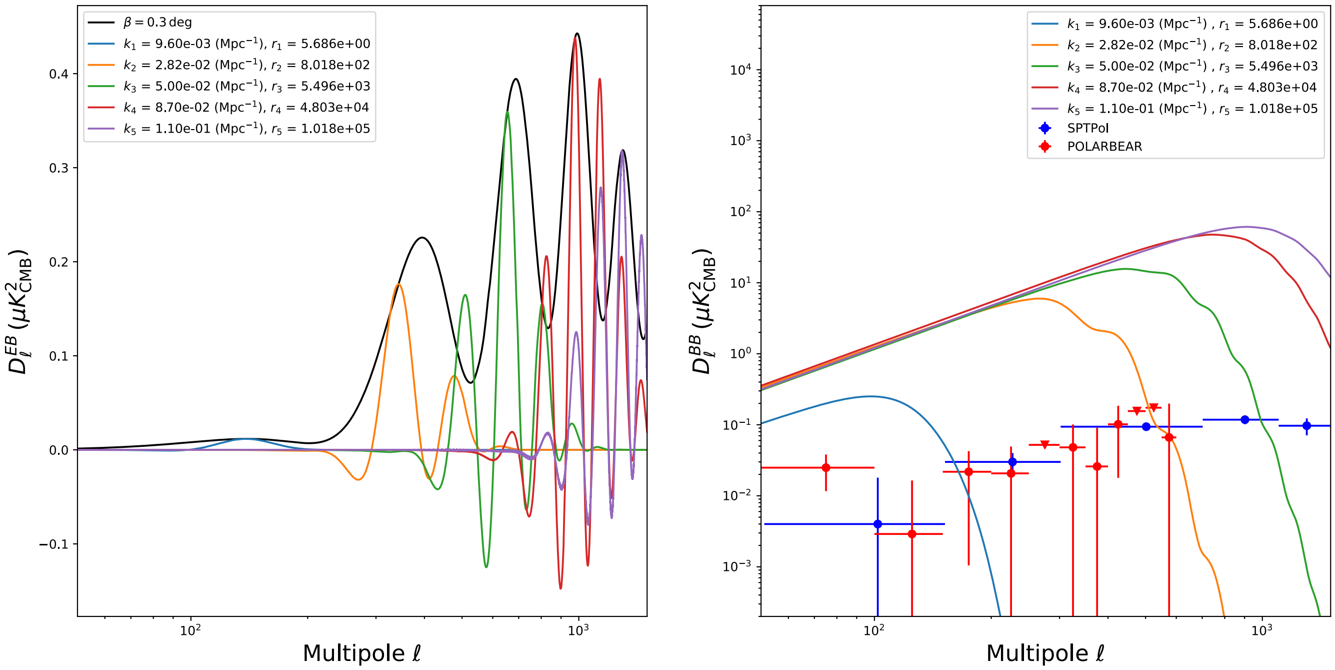

FIG. 1. Left panel: EB angular power spectra $D_\ell^{EB} \equiv \ell(\ell+1)C_\ell^{EB}/(2\pi)$ against multipole ℓ. The black line denotes D_ℓ^{EB} induced by cosmic birefringence with rotation angle of $\beta = 0.3$ deg and we try reproducing it. The other colored lines represent individual D_ℓ^{EB} contributions produced by each term in the CGW spectrum (1) with the parameters tuned to match the peaks of the black line. Right panel: BB angular power spectra D_ℓ^{BB} produced by the same CGWs as the left panel in the same color. Blue and red plots represent the actual BB power spectra observed by SPTPol and POLARBEAR, which include foreground emissions, and any D_ℓ^{BB} prediction above them should be excluded. Circle dots and vertical bars show central values and $1\sigma(68\%)$ uncertainties, respectively. For the plots with negative center values, we show 95% confidence level upper bound with inverted triangles.

parameters and we did not pursue such a fine-tuning, which would not affect our conclusion.

One might wonder if a similar multiple peak structure in the EB spectrum could be reproduced by the tensor transfer functions without superposing five different log-normal spectra of CGWs. However, a single wide CGW spectrum leads to a EB spectrum that has only a couple of peaks for $\ell \lesssim 200$ but no large peaks $\ell \gtrsim 600$ due to the highly damping nature of the tensor transfer function (see, e.g., [26,34,35]). Hence, it is difficult to reproduce these EB peaks without a tuning. Although it might be possible to find a suitable oscillating spectrum of CGWs, that would not impact on our conclusion drawn below.

IV. OVERPRODUCTION OF *BB* SPECTRUM

In this section, we consider a BB power spectrum that must be simultaneously produced through Eq. (2). Since CMB observations have measured the BB power spectrum for the relevant ℓ range, one should seek an appropriate parameter set of the CGWs, which does not produces a too large BB, while reproducing EB.

In the right panel of Fig. 1, the colored lines show the calculated BB spectra induced by the CGWs for the same sets of the CGW parameters as the previous section. The observed BB data taken by SPTPol [6] (blue points) and POLARBEAR [38] (red points) are also shown with error bars. From this panel, one can see that the induced BB spectra from the CGWs far exceed the measured amplitude and thus the corresponding parameters should be excluded. We note that even the blue line, which is adjusted to the first peak and has the smallest height, also overproduces the BB spectrum. This result implies that it is hard for the CGWs to explain the observed EB spectrum without conflicting with the observed BB.

We have fixed the width parameter σ for the CGWs as $\sigma = 0.2$ so far. Does a different value of σ alleviate the incompatibility between EB and BB? To test this possibility, we compute the ratio of the maximum value of D_ℓ^{BB} to that of D_ℓ^{EB} by increasing σ for each contribution in Eq. (1) separately. As is apparent from Fig. 1, since the peak height in the target D_ℓ^{EB} is a few times 0.1 $\mu\mathrm{K}^2_{\mathrm{CMB}}$ and the maximum value of the observed D_ℓ^{BB} is 0.24 $\mu\mathrm{K}^2_{\mathrm{CMB}}$, this ratio $\max[D_\ell^{BB}]/\max[D_\ell^{EB}]$ should be less than 2.4 at least. The result is shown in Fig. 2. Although the ratio changes depending on k_i, it never becomes smaller than 21.5 for $\sigma \geq 0.2$. For larger σ, the ratios converge to the same value around 36.5, because the CGW spectrum $\mathcal{P}_h^R$ becomes flatter and less dependent on its peak position k_i. Note that this ratio does not depend on r_i. Therefore, we find that larger σ does not mitigate the problem of the

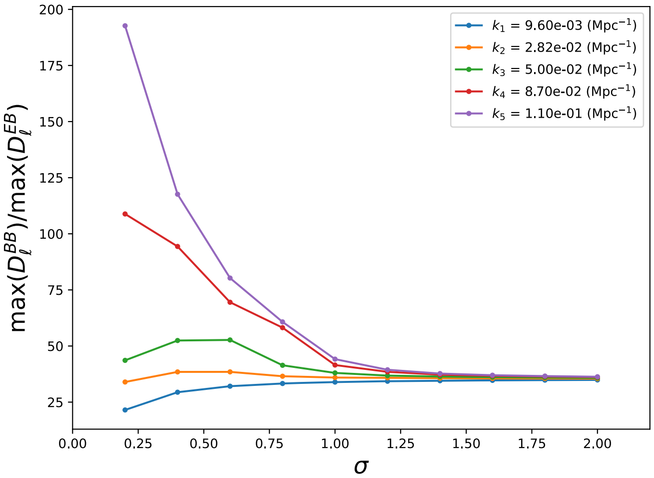

FIG. 2. Ratios of maximum D_ℓ^{BB} to maximum D_ℓ^{EB} against varied width parameter σ of $\mathcal{P}_h^R(k)$. The color scheme is the same as Fig. 1. The ratio is always larger than 21.5, while it should be at least smaller than 2.4 to explain the observed EB without overproducing the BB spectrum.

overproduction of BB spectrum. Even though we can make the $\max[D_\ell^{BB}]/\max[D_\ell^{EB}]$ ratio smaller with σ smaller than 0.2, the peaks of the EB spectrum from the CGWs would be too sharp to explain the target EB spectrum.

V. SUMMARY AND DISCUSSION

Recently, the EB power spectrum, which is well explained by cosmic birefringence with rotation angle $\beta \approx 0.3$ deg, has been observed in CMB data. In this paper, we investigated the possibility that this observed EB spectrum is produced by primordial CGWs instead of cosmic birefringence. However, we found that if CGWs produced a similar EB spectrum to the observed one, they would inevitably overproduce a BB spectrum whose amplitude is much larger than the measured value by SPTPol and POLARBEAR. Therefore, it is difficult to attribute the observed EB spectrum to CGWs.

To parametrize the CGW spectrum, we superposed five log-normal spectra with different peak heights and positions in Eq. (1) and analyzed it. Nonetheless, we expect that our conclusion does not depend on the detailed shape of the CGW spectrum, because the EB and BB spectra are linear function of $\mathcal{P}_h^R(k)$. Moreover, this CGW template enabled us to illustrate that even CGWs reproducing only one peak of the EB spectrum lead to overproduction of BB and should be excluded.

The reason for the difficulty of the CGW scenario can be understood as follows. The newly observed EB spectrum is smaller than the standard EE spectrum mainly contributed by the scalar perturbation by a factor of $C_\ell^{EB,\rm obs}/C_\ell^{EE,\rm scalar} = \sin(4\beta)/2 \approx 10^{-2}$ for $\beta \approx 0.3°$. On the other hand, it has been known that scale-invariant primordial gravitational waves produce the EE and BB spectra of roughly equal size, $C_\ell^{EE,\rm tens} \simeq C_\ell^{BB,\rm tens} \simeq 10^{-4} r C_\ell^{EE,\rm scalar}$, where and hereafter we consider $\ell \approx 600$, and r is the tensor-to-scalar ratio. Thus, we expect that CGWs produce a EB spectrum, $C_\ell^{EB,\rm tens} \simeq 10^{-2} r C_\ell^{EB,\rm obs}$, and in order to reproduce the observed EB spectrum, $r \simeq 10^2$ is necessary, which leads to $C_\ell^{BB,\rm tens} \simeq 10^{-2} C_\ell^{EE,\rm scalar}$. This is incompatible with an observed fact at $\ell \sim 600$ that $C_\ell^{BB,\rm obs} \simeq C_\ell^{BB,\rm lens} \simeq 10^{-3} C_\ell^{EE,\rm scalar}$ with $C_\ell^{BB,\rm lens}$ the lensing B-mode spectrum. Note that the above argument assumed scale-invariant CGWs and derived smaller amplitude parameter than $r_i \sim 10^3$ obtained in Sec. III. Nonetheless, it illustrates the basic reason why CGWs cause the incompatibility between the EB and BB spectra.

In this paper, we did not study the case with an extremely small width parameter, $\sigma < 0.2$. The trend in Fig. 2 infers that smaller σ would increase the ratio, $\max[D_\ell^{BB}]/\max[D_\ell^{EB}]$, for the fourth (red) and fifth (purple) peaks and thus worsen the conflict between EB and BB. Even if the ratio decreases for much smaller σ, such a spikelike D_ℓ^{EB} would not be responsible for the entire observed EB spectrum. While a dedicated analysis should be done to rigorously dismiss this possibility, we expect that smaller σ would not give a viable solution.

Finally, we note that the target EB spectrum in Fig. 1 that we tried to reproduce is not the actual observed data but is obtained based on the interpretation of cosmic birefringence. It is possible that the EB spectra from the CGWs fits the actual data better than the birefringence model. Even in that case, CGWs with similar amplitude should be required and hence the overproduction of the BB spectrum would remain as a generic problem, which would exclude the CGWs scenario.

ACKNOWLEDGMENTS

This work was supported in part by Japan Society for the Promotion of Science (JSPS) KAKENHI, Grants No. JP18K13537 (T. F.), No. JP20H05854 (T. F.), No. JP20H01932 (S. Y.), No. JP20K03968 (S. Y.), No. JP20K14497 (Y. M.), No. JP19K14718 (M. S.), and No. JP20H05859 (M. S.). The authors thank the Yukawa Institute for Theoretical Physics at Kyoto University. Discussions during the YITP workshop YITP-T-21-08 on "Upcoming CMB observations and Cosmology" were useful to complete this work. The authors are grateful to Yuji Chinone for suggestions on the plots of power spectra. M. S. acknowledges the Center for Computational Astrophysics, National Astronomical Observatory of Japan, for providing the computing resources of Cray XC50.

[1] E. Komatsu *et al.* (WMAP Science Team Collaboration), Results from the Wilkinson Microwave Anisotropy Probe, Prog. Theor. Exp. Phys. **2014**, 6B102 (2014).

[2] Planck Collaboration VI, Planck 2018 results. VI. Cosmological parameters, Astron. Astrophys. **641**, A6 (2020).

[3] S. Adachi *et al.* (POLARBEAR Collaboration), Improved upper limit on degree-scale CMB B-mode polarization power from the 670 square-degree POLARBEAR survey, Astrophys. J. **931**, 101 (2022).

[4] S. Adachi *et al.* (POLARBEAR Collaboration), A measurement of the CMB *E*-mode angular power spectrum at subdegree scales from670 square degrees of POLARBEAR data, Astrophys. J. **904**, 65 (2020).

[5] S. Aiola *et al.* (ACT Collaboration), The Atacama Cosmology Telescope: DR4 maps and cosmological parameters, J. Cosmol. Astropart. Phys. 12 (2020) 047.

[6] J. T. Sayre *et al.* (SPT Collaboration), Measurements of B-mode polarization of the cosmic microwave background from 500 square degrees of SPTpol data, Phys. Rev. D **101**, 122003 (2020).

[7] D. Dutcher *et al.* (SPT-3G Collaboration), Measurements of the E-mode polarization and temperature-E-mode correlation of the CMB from SPT-3G 2018 data, Phys. Rev. D **104**, 022003 (2021).

[8] P. A. R. Ade *et al.* (BICEP, Keck Collaborations), Improved Constraints on Primordial Gravitational Waves using Planck, WMAP, and BICEP/Keck Observations through the 2018 Observing Season, Phys. Rev. Lett. **127**, 151301 (2021).

[9] P. A. R. Ade *et al.* (SPIDER Collaboration), A constraint on primordial *B*-modes from the first flight of the SPIDER Balloon-Borne Telescope, Astrophys. J. **927**, 174 (2022).

[10] Y. Minami and E. Komatsu, New Extraction of the Cosmic Birefringence from the Planck 2018 Polarization Data, Phys. Rev. Lett. **125**, 221301 (2020).

[11] P. Diego-Palazuelos *et al.*, Cosmic Birefringence from the Planck Data Release 4, Phys. Rev. Lett. **128**, 091302 (2022).

[12] J. R. Eskilt and E. Komatsu, Improved constraints on cosmic birefringence from the WMAP and Planck cosmic microwave background polarization data, Phys. Rev. D **106**, 063503 (2022).

[13] Y. Minami, H. Ochi, K. Ichiki, N. Katayama, E. Komatsu, and T. Matsumura, Simultaneous determination of the cosmic birefringence and miscalibrated polarization angles from CMB experiments, Prog. Theor. Exp. Phys. **2019**, 083E02 (2019).

[14] J. R. Eskilt, Frequency-dependent constraints on cosmic birefringence from the LFI and HFI Planck Data Release 4, Astron. Astrophys. **662**, A10 (2022).

[15] T. Fujita, K. Murai, H. Nakatsuka, and S. Tsujikawa, Detection of isotropic cosmic birefringence and its implications for axionlike particles including dark energy, Phys. Rev. D **103**, 043509 (2021).

[16] F. Takahashi and W. Yin, Kilobyte cosmic birefringence from ALP domain walls, J. Cosmol. Astropart. Phys. 04 (2021) 007.

[17] L. W. H. Fung, L. Li, T. Liu, H. N. Luu, Y.-C. Qiu, and S. H. H. Tye, Axi-Higgs cosmology, J. Cosmol. Astropart. Phys. 08 (2021) 057.

[18] G. Choi, W. Lin, L. Visinelli, and T. T. Yanagida, Cosmic birefringence and electroweak axion dark energy, Phys. Rev. D **104**, L101302 (2021).

[19] I. Obata, Implications of the cosmic birefringence measurement for the axion dark matter search, J. Cosmol. Astropart. Phys. 09 (2022) 062.

[20] S. Gasparotto and I. Obata, Cosmic birefringence from monodromic axion dark energy, J. Cosmol. Astropart. Phys. 08 (2022) 025.

[21] A. Lue, L.-M. Wang, and M. Kamionkowski, Cosmological Signature of New Parity Violating Interactions, Phys. Rev. Lett. **83**, 1506 (1999).

[22] S. Alexander and J. Martin, Birefringent gravitational waves and the consistency check of inflation, Phys. Rev. D **71**, 063526 (2005).

[23] T. Takahashi and J. Soda, Chiral Primordial Gravitational Waves from a Lifshitz Point, Phys. Rev. Lett. **102**, 231301 (2009).

[24] M. M. Anber and L. Sorbo, Non-Gaussianities and chiral gravitational waves in natural steep inflation, Phys. Rev. D **85**, 123537 (2012).

[25] P. Adshead and M. Wyman, Chromo-Natural Inflation: Natural Inflation on a Steep Potential with Classical Non-Abelian Gauge Fields, Phys. Rev. Lett. **108**, 261302 (2012).

[26] R. Namba, M. Peloso, M. Shiraishi, L. Sorbo, and C. Unal, Scale-dependent gravitational waves from a rolling axion, J. Cosmol. Astropart. Phys. 01 (2016) 041.

[27] I. Obata and J. Soda, Chiral primordial gravitational waves from dilaton induced delayed chromonatural inflation, Phys. Rev. D **93**, 123502 (2016); **95**, 109903(E) (2017).

[28] E. Dimastrogiovanni, M. Fasiello, and T. Fujita, Primordial gravitational waves from axion-gauge fields dynamics, J. Cosmol. Astropart. Phys. 01 (2017) 019.

[29] P. Adshead and E. I. Sfakianakis, Higgsed gauge-flation, J. High Energy Phys. 08 (2017) 130.

[30] T. Fujita, E. I. Sfakianakis, and M. Shiraishi, Tensor spectra templates for axion-gauge fields dynamics during inflation, J. Cosmol. Astropart. Phys. 05 (2019) 057.

[31] C. S. Machado, W. Ratzinger, P. Schwaller, and B. A. Stefanek, Audible axions, J. High Energy Phys. 01 (2019) 053.

[32] E. McDonough and S. Alexander, Observable chiral gravitational waves from inflation in string theory, J. Cosmol. Astropart. Phys. 11 (2018) 030.

[33] O. Iarygina and E. I. Sfakianakis, Gravitational waves from spectator Gauge-flation, J. Cosmol. Astropart. Phys. 11 (2021) 023.

[34] J. R. Pritchard and M. Kamionkowski, Cosmic microwave background fluctuations from gravitational waves: An analytic approach, Ann. Phys. (Amsterdam) **318**, 2 (2005).

[35] B. Thorne, T. Fujita, M. Hazumi, N. Katayama, E. Komatsu, and M. Shiraishi, Finding the chiral gravitational wave background of an axion-SU(2) inflationary model using CMB observations and laser interferometers, Phys. Rev. D **97**, 043506 (2018).

[36] A. Lewis, A. Challinor, and A. Lasenby, Efficient computation of CMB anisotropies in closed FRW models, Astrophys. J. **538**, 473 (2000).

[37] https://camb.info/.

[38] S. Adachi *et al.* (POLARBEAR Collaboration), A measurement of the degree scale CMB *B*-mode angular power spectrum with POLARBEAR, Astrophys. J. **897**, 55 (2020).